LA-UR- 04-0778

Approved for public release;
distribution is unlimited.

Title: Heterogeneity in Texture Development in Single Pass Equal Channel Angular Extrusion

Author(s):
Irene J. Beyerlein, T-3
Saiyi Li, MST-8
David J. Alexander,MST-6
Carl T. Necker, MST-6
Carlos N. Tome, MST-8
Mark Bourke, MST-8

Submitted to:
TMS Society 2004
Charlotte NC
March 14-19, 2004

Los Alamos
NATIONAL LABORATORY

HETEROGENEITY IN TEXTURE DEVELOPMENT IN SINGLE PASS EQUAL CHANNEL ANGULAR EXTRUSION

***Irene J. Beyerlein*, ***Saiyi Li, **David Alexander,
**Carl Necker, ***Carlos Tome, ***Mark Bourke

*T-3, **MST-6, ***MST-8, Los Alamos National Laboratory

To be presented at

TMS Society 2004
Charlotte NC
March 14-19, 2004

Proceedings: **Ultrafine Grained Materials**

ABSTRACT

We investigate inhomogeneity in deformation of OFE Cu in a single pass of Equal Channel Angular Extrusion (ECAE). A finite element simulation of the rounded corner die used here shows that deformation occurs primarily over a broad region with an exception of low shear deformation in the round corner region. An analytical model for the deformation history induced by this two-part deformation zone is imported into a viscoplastic self-consistent (VPSC) polycrystalline model for texture prediction. Orientation Image Microscopy (OIM) measurements show that the texture evolution varies from top to the middle by a slight rotation and that the bottom region experiences little deformation but large rotations. Texture predictions agree reasonably well with these OIM measurements in features and intensity.

.

This work was carried out under the auspices of the National Nuclear Security Administration of the U.S. Department of Energy at Los Alamos National Laboratory under Contract No. W-7405-ENG-36.

Ultrafine Grained Materials III *Edited by Y.T. Zhu, T.G. Langdon, R.Z. Valiev, S.L. Semiatin, D.H. Shin, and T.C. Lowe.* **TMS (The Minerals, Metals & Materials Society), 2004**

HETEROGENEITY IN TEXTURE DEVELOPMENT IN SINGLE PASS EQUAL CHANNEL ANGULAR EXTRUSION

I. J. Beyerlein[1,*], S. Li[2], D. J. Alexander[2], C. T. Necker[2], C. N. Tomé[2], and M. A. Bourke[2]
[1]Theoretical Division and [2]Materials Science and Technology Division,
Los Alamos National Laboratory, Los Alamos, NM 87545

Abstract

We investigate inhomogeneity in deformation of OFE Cu in a single pass of Equal Channel Angular Extrusion (ECAE). A finite element simulation of the rounded corner die used here shows that deformation occurs primarily over a broad region with an exception of low shear deformation in the round corner region. An analytical model for the deformation history induced by this two-part deformation zone is imported into a viscoplastic self-consistent (VPSC) polycrystalline model for texture prediction. Orientation Image Microscopy (OIM) measurements show that the texture evolution varies from top to the middle by a slight rotation and that the bottom region experiences little deformation but large rotations. Texture predictions agree reasonably well with these OIM measurements in features and intensity.

Keywords: Copper, finite element, flow pattern, polycrystalline modeling

Introduction

Equal Channel Angular Extrusion (ECAE) [1] is an attractive process as it can potentially produce low porosity, nano-structured metals in bulk with an extraordinary combination of mechanical properties: ultra high strength, high ductility and superplastic forming behavior [2]. However the concomitant high strength and ductility observed in some ECAE materials challenge conventional ideas of deformation mechanisms in metals. In addition, there is great flexibility in the processing and sensitivity to multiple processing and material parameters. As a consequence, reliable simulation techniques constitute a desirable tool for exploring the myriad of processing options without having to build the tools and/or perform the experiments.

ECAE [1] is a discontinuous process, involving inserting and re-inserting a sample into a die (See Fig. 1), which contains two channels with equal cross-section, intersecting at an angle Φ. As it is forced to pass through the die, the sample is severely deformed in shear as it changes its direction by the die angle Φ, starting as low as 90°. The sample cross-section undergoes no change in shape and therefore the sample can be re-inserted into the die to accumulate more strain. Reinsertion changes the strain path and rotating the billet either counterclockwise (CCW) or clockwise (CW) after each extrusion provides further variations in strain path.

ECAE deformation during a single pass has been described as simple shear along the intersection plane of the entry and exit die. This ideal viewpoint is approached when the inner and outer corners are sharp, frictionless conditions exist, backpressure is applied, and the material is rigid plastic [3,4]. In this view, when $\Phi = 90°$ as in Fig. 1, the sample accumulates an equivalent plastic strain of 1.15 per pass. However in most cases, plastic deformation occurs over a much broader region, whose shape depends sensitively on several factors, such as

* Corresponding Author. irene@lanl.gov

contact friction, material flow response, backpressure, pressing rate, and die design. In general, these plastic deformation zones induce inhomogeneous deformation in the sample.

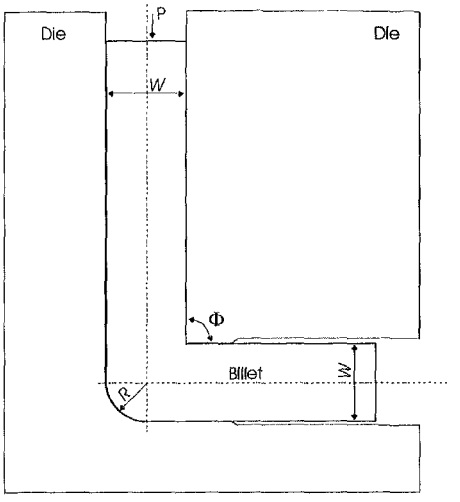

Figure 1. Schematic of the ECAE die

Inhomogeneous deformation during each pass suggests the possibility of heterogeneity in the final microstructure and texture of the material and hence mechanical properties across the sample. Our approach will be to numerically and analytically model the essential deformation characteristics for different material points and import the deformation history into a polycrystalline model for microstructure, texture, and mechanical response prediction.

In this paper, we investigate the inhomogeneity in deformation and in texture development during a single ECAE pass of copper. The tooling has a rounded corner and was well lubricated. Using a 2-D finite element (FE) model of our die [5], we simulate a single ECAE pass and investigate the plastic deformation zone that forms and the inhomogeneity in the final strain. We then model analytically the associated deformation history [6] and import it into a visco-plastic self-consistent (VPSC) polycrystalline model [7,8] to relate the shape of the plastic deformation zone and texture evolution. VPSC model predictions were compared with Orientation Image Microscopy (OIM) texture measurements at different points in the sample.

Approach

ECAE Processing

The copper was commercially procured C10100 (OFE purity) rod 9.5 mm (or 0.375 in.) in diameter, in the H80 fully drawn condition. Portions of the rod, approximately 100 mm in length, were first cleaned in nitric acid, and then annealed for 1 h at 550°C in an atmosphere of Ar-6 H gas. This heat treatment produced an equiaxed grain size of about 50 μm.

A schematic of our ECAE die is shown in Fig. 1. The angle between the inlet and outlet channels Φ was 90°. The tooling for the ECAE was fabricated from H13 tool steel, which was heat-treated to R_C 58. The die was 63.5 x 63.5 x 152.4 mm (2.5 x 2.5 x 6 in.) in size, with an inlet channel diameter of 9.5 mm (0.375 in.). To simplify fabrication, the outer corner radius R at the intersection of the inlet and outlet channels was 4.8 mm (0.188 in.), or half the inlet channel diameter. As shown in Fig. 1, 5.1 mm (0.20 in.) from the inner corner, the outlet channel was slightly smaller in diameter (9.3 mm [0.368 in.]), so that the processed billet could be easily re-inserted into the inlet channel. Beyond 5.1 mm, the outer channel then expanded to 9.8 mm (0.386 in.) in diameter to reduce the surface area over which friction acts.

The billet was 9.5 mm (0.375 in.) in diameter and ~50 mm (2 in.) in length. The billet and tooling were lubricated with a MoS_2-containing grease (Jet-Lube 550 Anti-Seize Lubricant, Jet-Lube, Houston, TX). A short plug approximately 19 mm (0.75 in.) long of C11000 copper was inserted in the die inlet channel at the tail of the billet. The billet was extruded at room temperature at a ram speed of 6.35 mm/s (0.25 in./s). The plug at the billet tail allowed the billet to be pushed through the die corner and beyond the outlet channel land without interruption. This allowed the billet to be removed from the die at the completion of the ram stroke. The plug remained in the die corner, and was expelled by the next extrusion.

OIM Measurement

Samples for microtexture analysis were prepared using standard metallographic preparation techniques through a final polish with colloidal silica. Samples were electro-polished in a 50/50 orthophosphoric/DI water mixture for a few seconds, rinsed in water and then alcohol. Microtextures were measured on a Phillips XL30 environmental scanning electron microscope equipped with TSL hardware and software. A series of scans 1 mm high, 0.5 mm wide were made from the top to bottom surfaces of the material prepared with the extrusion axis normal to the sample surface. These scans were performed consecutively so as to not induce any sample rotations typical of removing and then re-staging samples. The step size was 5 μm. The TSL dilation clean-up feature was used to dissolve single and paired points into the surrounding data with misorientations greater than 15° from all neighboring points. Textures were calculated for (111), (110) and (100) poles. The OIM data was reduced into grain files where each grain is defined by a single orientation and boundary misorientations exceeding 5°. This reduction in data allowed for comparative plots with the VPSC model textures.

FE Modeling

FE simulations [5] were carried out using ABAQUS [9]. The die and the ram are modeled with analytically rigid surfaces. Plane strain and frictionless sliding between the billet and tooling are assumed. The material model for the billet is elasto-perfectly plastic with a yield stress of 31 MPa, a Young's modulus of 110 GPa and a Poisson's ratio of 0.35. The inlet and outlet channels, and billet width, W, are equal and set to 9.35 mm, the width of the outlet channel of the actual tooling. The length of the billet and inlet channel are 83 mm and 88 mm, respectively, such that the billet is fully accommodated in the channel at the start of the ECAE process. Like the actual tooling, the outlet channel has a land and a relief with the same dimensions. The outer radius R is $0.5W$ and inner radius is 0.25 mm. ECAE was simulated by using a flat-faced ram to push the billet through the die for a total displacement of 63.5 mm in 10 s. The billet length and ram displacement adopted here were expected to be long enough to obtain a well-defined steady-state region in the billet after deformation. The entire FE model used 3569 four-node plane strain elements (21 elements across W) with linear integration.

Analytical Flow Modeling

We consider deformation to occur over a broad region as the material passes through the corner of the die, building on the slip fields determined by Segal [4] for round corner dies. In [6], we determined the velocity gradient, in fixed global coordinates, for the two-part plastic deformation zone shown in Fig. 2, which consists of a central fan AOB and an outer rotating region ABCD. The location of the inner corner of the die is assigned (O_x, O_y). Any given flow line begins at time $t = 0$ and at $X = (x_0, y_0, z_0)$ inside the die. The magnitude of the velocity of the material in the entry and exit die is V (not necessarily the ram velocity). This two-part zone is likely to be generated when either a free surface (or corner gap) forms in the outer corner or

the die itself has a rounded corner. In the former case, friction and material response play a larger role in determining the plastic deformation zone shape [3,10], whereas in the latter case with use of a rounded die, the tooling largely dictates the plastic deformation zone shape. A flow line along the boundary of the two parts is considered to deform as if it were part of the upper region.

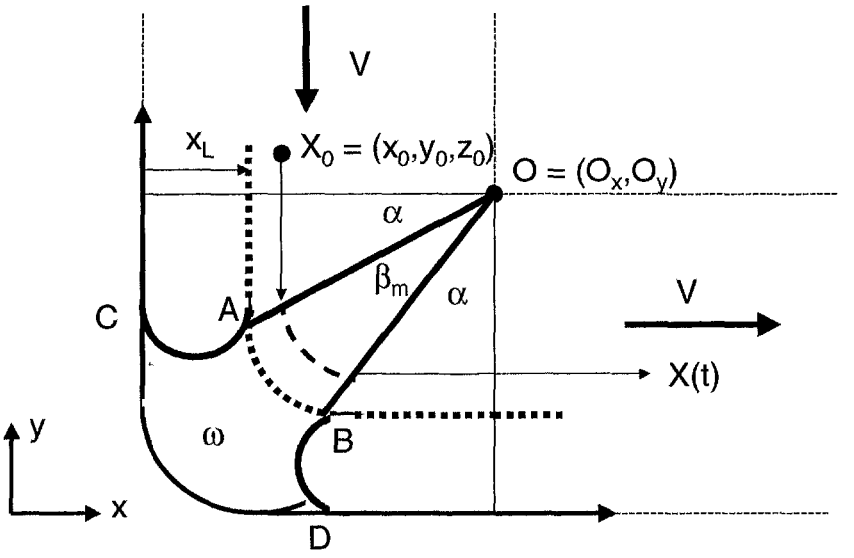

Figure 2. Schematic of the two-part plastic deformation zone used in analytical flow model.

For this two-part plastic zone, deformation is inhomogeneous as it depends on the location of the material point. First we consider material points flowing through the fan in the upper region. As shown in Fig. 2, the central fan AOB is centered at the corner of the die by an angle α from both sides. α can adopt values from 0 to $\pi/4$, and is constant. By geometry, the inner angle of the fan β_m, is $\beta_m = \pi/2 - 2\alpha$, which ranges from 0 to $\pi/2$ as α decreases from $\pi/4$ to 0. Material points within the fan reach the first boundary of the fan OA at time t_1,

$$t_1 = \frac{(y_0 - O_y) + (O_x - x_0)\tan\alpha}{V} \tag{1}$$

The material reaches the outer boundary OB at time t_2.

$$t_2 = \frac{1}{V}\left[(y_0 - O_y) + (O_x - x_0)\tan\alpha + \frac{\beta_m (O_x - x_0)}{\cos^2\alpha}\right] \tag{2}$$

We find it convenient to introduce a scaling factor for time t,

$$t_n = \frac{(O_x - x_0)}{V} \tag{3}$$

Applying (3) to time constants t_1 and t_2 as follows

$$t_1^* = \frac{t'}{t_n} = \frac{t - t_1}{t_n} \quad \text{and} \quad t_2^* = \frac{t_2 - t_1}{t_n} = \frac{\beta_m}{\cos^2\alpha} \tag{4}$$

renders them dimensionless. The normalized expression for $\bar{\beta}(t^*)$, the angular position of the material as it flows through the fan, is

$$\bar{\beta}(t^*) = \beta(t) = t_1^* \cos^2\alpha \tag{5}$$

Applying these normalizations to our derivation of the velocity gradient L [6], we obtain the normalized $\bar{L}$, in the 1-2-3 coordinate system in Fig. 2. $\bar{L}$ varies only with angle $\bar{\beta}(t^*)$ as

$$\bar{L} = t_n L = \cos^2\alpha \begin{bmatrix} \frac{\sin 2(\alpha+\bar{\beta})}{2} & -\cos^2(\alpha+\bar{\beta}) & 0 \\ \sin^2(\alpha+\bar{\beta}) & -\frac{\sin 2(\alpha+\bar{\beta})}{2} & 0 \\ 0 & 0 & 0 \end{bmatrix} \tag{6}$$

Significantly, the form of $\bar{L}$ only depends on α and β, but not on $X = (x_0, y_0, z_0)$ or V. As α decreases from $\pi/4$ to 0, the differences in the magnitudes of the components increase, which as we will show later, influences texture evolution.

In the lower region, the material experiences substantially less deformation. The slip field analysis of Segal [4] obtained for a rounded corner describes the deformation in the lower region as shear deformation and rotation. We adopt this interpretation and obtain in [6] the corresponding velocity gradient. Generally for material points flowing through the lower region, we assume that the material experiences localized shear deformation when crossing boundaries AC and BD and travels from AC to BD via a rigid body rotation about O with rotational velocity ω.

$$\omega \approx \frac{V\cos^2(\pi/4 - \Psi/2)}{(O_x - x_0)} \tag{7}$$

As in our case when the material fills the die, AC and BD correspond to the discontinuity in the tooling, where the outer curvature mates with the entry and exit channels.

Visco-Plastic Self-Consistent (VPSC) Polycrystal Modeling

We are currently developing a modeling framework for predicting the macroscopic viscoplastic deformation, microstructural evolution and texture evolution in polycrystalline materials during the ECAE process [8]. We choose to build this framework using the VPSC model [7] to provide the interaction between individual grains and the polycrystalline aggregate. To elucidate the relationship between the plastic deformation zone and texture evolution, the following selections in applying VPSC are made. First the model polycrystal is single phase with a face-centered cubic (FCC) crystal structure. The starting material imports the same weak initial wire drawn texture as measured by OIM (See Fig. 5a) and has spherical grains. We also assume that the critical resolved shear stress for slip in the single FCC crystal is constant, without hardening by dislocation activity. Second, we employ an empirical grain subdivision law [8]. These criteria are designed such that when the grain becomes severely elongated or flat, it is fragmented into two or four equal parts, respectively. Thirdly, we

implement a grain-grain interaction scheme [11], which has proven to slow down the texture evolution and provide better agreement with texture measurements [12,13].

Results

Finite Element Modeling

Figure 3 shows the FE results for equivalent strain. As shown, the material completely fills the die. In the steady state region of the exit channel, we find that deformation is homogeneous in the center of the sample but is non-uniform in the top and bottom layers (~18% from the top and bottom surfaces) of the sample and in the head-end of the sample, ~1.5W in length. Figure 4 shows the equivalent Von Mises strain rate $\overline{D}$ and normal strain rate D_{11} in the 1-direction in order to expose the plastic deformation zone. Even in this frictionless case, plastic deformation is shown to occur over a broad region due to the rounded corner. This plastic deformation zone has approximately a fan shape with the exception of the lower 10% in the rounded corner region. Estimating a corresponding value of α for the upper region is, however, not straightforward and would require selecting a minimum value of $\overline{D}$ to define the boundary of the fan. If we were to select say $\overline{D}$ = 0.8 1/s, then the α obtained from Fig. 4a would be smaller in the top region than in the middle.

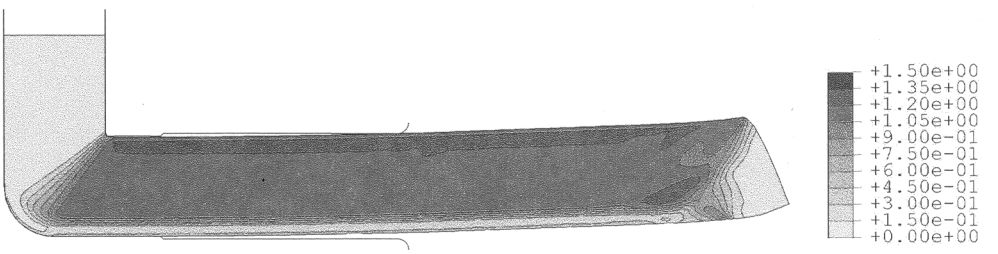

Figure 3. FE results for equivalent plastic strain in single pass of ECAE die in Fig. 1.

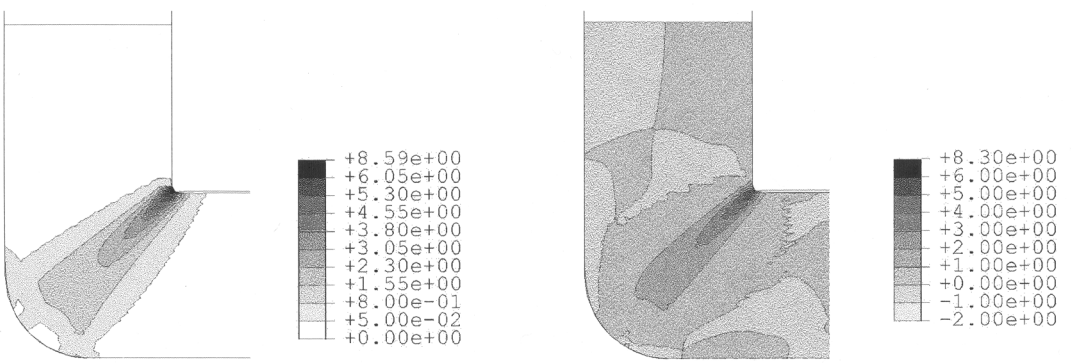

Figure 4. FE results for (a) equivalent strain rate and (b) strain rate in 1-direction, D_{11}.

Texture Evolution

Figure 5 compares the OIM texture measurements (Fig. 5b) with the VPSC texture predictions (Fig. 5c) using Eqn (6) for the imposed velocity gradient for a single ECAE pass. These (111) pole figures are oriented in the 1-2 plane of the die (See Fig. 2). OIM texture measurements for the bottom, middle, and top correspond respectively to scans within 1 mm from the bottom, in the center, and within 1 mm from the top. These measurements show that the sample textures vary from top to bottom. While both the top and middle textures have the characteristic six

spoke shear texture, they differ by a rotation about the 3-axis and in intensity, with the mid-line texture being more intense. The bottom texture is distinctly different than the top and middle textures. Compared to the initial wire drawn texture (Fig. 5a), the bottom texture is slightly more intense (3.2 vs 4.1 muliple of random orientation (m.r.o.)) and rotated about the 3-axis.

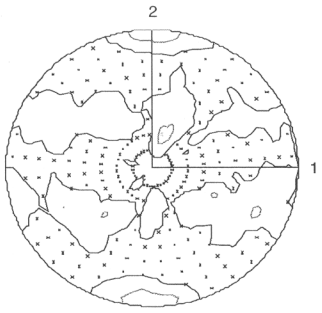

(a) Initial wire drawn texture

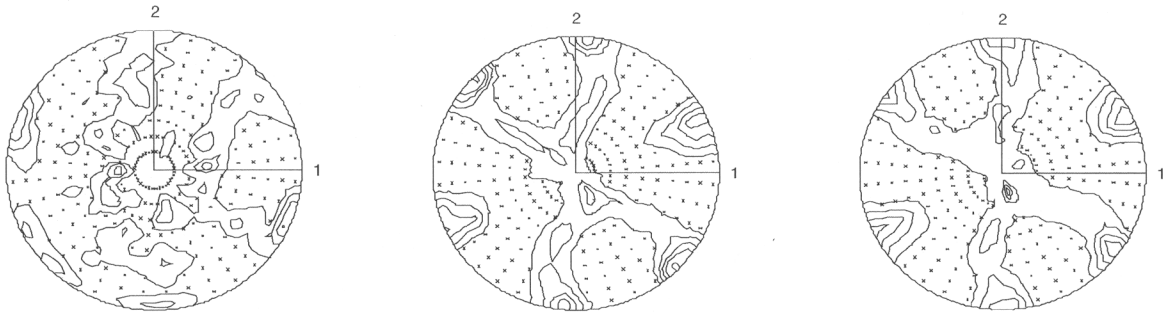

(b) OIM measurement, BOTTOM MIDDLE TOP

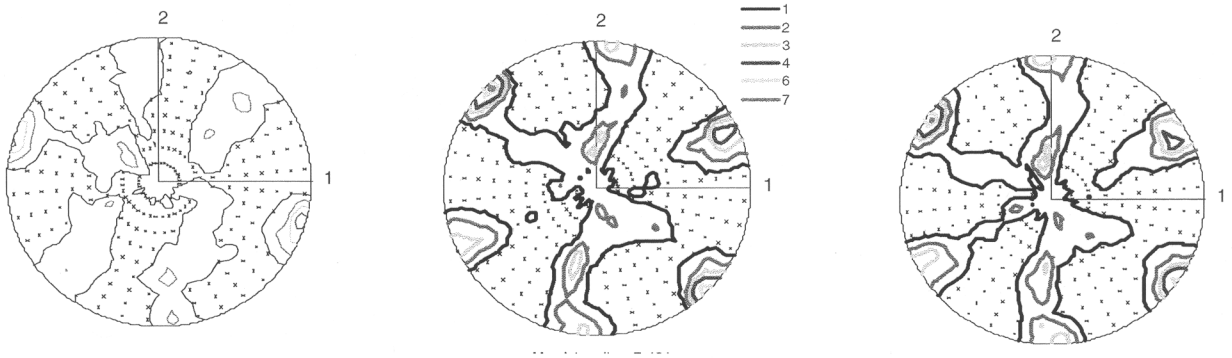

(c) VPSC predictions, BOTTOM MIDDLE TOP

Figure 5. (111) pole figures of (a) OIM measured initial texture in Cu (b) OIM measured textures after one pass in the top, middle and bottom regions and (c) corresponding VPSC texture predictions. Level lines for all pole figures correspond to 1, 2, 3, 4, 6, and 7 m.r.o. The maximum intensity for the initial wire drawn texture is 3.2. The maximum intensities for the top, middle and bottom OIM measurements are 5.3, 6.5, and 4.1 m.r.o, respectively. The maximum intensities for the top (α=28°), middle (α=36°) and bottom texture predictions are 7.2, 7.5, and 4.8 m.r.o, respectively.

Using our model, we find that texture evolution is sensitive to α of the central fan [6]. As α decreases from $\pi/4$ to 0, i.e. the fan broadens, the (111) pole figures in the 1-2 plane are rotated counter-clockwise about the 3-direction and the intensities of the maxima are altered. Therefore, by comparing texture measurement to prediction, we can characterize a value for α

for the top and middle points, that is, material points flowing through the fan. We have done so to produce texture predictions in Fig. 5c and find that the value of α is lower in the top than in the middle, being α = 28° and 36°, respectively. This trend coincides with what could be estimated from FE simulation results in Fig. 4a. Interestingly, with these values of α, the maximum intensity in the predicted textures increases from the top to the middle in agreement with those of the measurements (See Fig. 5 caption). Also, the features of these textures agree quite well, though the intensities are higher in the model. If α of the plastic zone were constant, then deformation for points flowing through the fan would be homogeneous. Thus this ECAE single pass deformation was inhomogeneous from top to bottom.

For the rounded corner regions, we feed our model the velocity gradient in [6] and ω of Eqn (7) into the VPSC code and find that it predicts similar texture features and intensities to that measured (See Fig. 5c). This agreement suggests that the low shear deformation and rigid rotation model for the rounded corner is a reasonable representation.

Conclusions

Deformation in our rounded ECAE die was found to be inhomogeneous and to lead to a non-uniform texture evolution across the copper sample in one pass. We show in this work that the deformation history can be described well by a two-part deformation zone, consisting of a central fan in the upper region and a rotating low deformation zone in the lower corner region. We find through FE simulations and model interpretations of the texture measurements that in reality the angle of the fan, controlled by a single parameter α, is not constant. Consequently, the top and middle texture differ by a rotation about the 3-axis (Fig. 2) and also in intensity. The values of α obtained from direct interpretation of the OIM texture measurements seem to coincide with those from our FE simulation model, which assumed a perfectly plastic material and frictionless conditions. Lastly, the FE, OIM, and VPSC texture predictions all suggest that the bottom ~10%-20% of the sample experiences substantially lower shear deformation and relatively large rotations.

Acknowledgements

This study was supported by a Los Alamos Laboratory-Directed Research and Development Project (no. 2003216).

References

1. V. M. Segal, V. I. Reznikov, A. E. Drobyshevski, V. I. Kopylov, *Russ Metall*, 1 (1981), 99-105.
2. R. Z. Valiev, I. V. Islamgaliev, I. V. Alexandrov, Prog. Mater. Sci., 45 (2000), 103.
3. J.-W. Park, J.-Y. Suh, *Metall Mater Trans A*, 32A (2001) 3007-3014.
4. V. M. Segal, Mat. *Sci. Engng*, A345 (2003), 36-46.
5. S. Li, I.J. Beyerlein, M.A.M. Bourke, C.N. Tomé, S.C. Vogel, D.W. Brown, B. Clausen, D.J. Alexander , In preparation (2003).
6. I. J. Beyerlein, C. N. Tomé. In preparation. (2003)
7. R. A. Lebensohn, C. N. Tomé, *Acta Metall. Mater.* 41 (1993) 2611.
8. I. J. Beyerlein, C. N. Tomé, R. A.Lebensohn, *Mater. Sci. Engng*. A345 (2003) 122-138.
9. ABAQUS User's Manual, Version 6.3, Hibbitt, Karlsson & Sorensen, Inc., (2002).
10. H. S. Kim, H. H. Seo, S. I. Hong, *Mat. Sci. Engng*. A291, (2000), 86-90.
11. C. N. Tomé, R. A. Lebensohn, C. T. Necker, *Metall Mater Trans A* 33 (2002), 2635-48.
12. S. Vogel, I. J. Beyerlein, M. A. M. Bourke, D. W. Brown, C. N. Tomé, T. G. Langdon, Cheng Xu, *Mater Sci Forum*, 408-412 (2002), 673-678.
13. S. C. Vogel, D. J. Alexander, I. J. Beyerlein, M. A. M. Bourke, D. W. Brown, B. Clausen, C. N. Tomé, R. B. Von Dreele, C. Xu, T. G. Langdon, *Mater Sci Forum*, 426-432 (2003), 2661.